



HHS Public Access

Author manuscript

Biosens Bioelectron. Author manuscript; available in PMC 2020 April 15.

Published in final edited form as:

Biosens Bioelectron. 2019 April 15; 131: 119–127. doi:10.1016/j.bios.2019.01.056.

Rapid quantification of two chemical nerve agent metabolites in serum

Michael Kammer¹, Amanda Kussrow¹, Melissa D. Carter², Samantha L. Isenberg², Rudolph C. Johnson², Robert H. Batchelor³, George W. Jackson³, and Darryl J. Bornhop¹

¹Department of Chemistry, Vanderbilt University, Nashville, TN, 37615, USA

²Centers for Disease Control and Prevention, Atlanta, GA, 30341, USA

³Base Pair Biotechnologies, Pearland, TX, 77584, USA

Abstract

Organophosphorus compounds (OPs) continue to represent a significant chemical threat to humans due to exposures from their use as weapons, their potential storage hazards, and from their continued use agriculturally. Existing methods for detection include ELISA and mass spectrometry. The new approach presented here provides an innovative first step toward a portable OP quantification method that surmounts conventional limitations involving sensitivity, selectivity, complexity, and portability. DNA affinity probes, or aptamers, represent an emerging technology that, when combined with a mix-and-read, free-solution assay (FSA) and a compensated interferometer (CI) can provide a novel alternative to existing OP nerve agent (OPNA) quantification methods. Here it is shown that FSA can be used to rapidly screen prospective aptamers in the biological matrix of interest, allowing the identification of a ‘best-in-class’ probe. It is also shown that combining aptamers with FSA-CI enables quantification of the OPNA metabolites, Sarin (NATO designation “G-series, B”, or GB) and Venomous Agent X (VX) acids, rapidly with high selectivity at detection limits of sub-10 pg/mL in 25% serum (by volume in PBS). These results suggest there is potential to directly impact diagnostic specificity and sensitivity of emergency response testing methods by both simplifying sample preparation procedures and making a benchtop reader available for OPNA metabolite quantification.

Keywords

Interferometry; Free Solution Assay; Organophosphorus Nerve Agents; Aptamers

*Corresponding author: Darryl.bornhop@vanderbilt.edu.

Disclaimer

The findings and conclusions in this study are those of the authors and do not necessarily represent the views of the U.S. Department of Health and Human Services, or the U.S. Centers for Disease Control and Prevention. Use of trade names and commercial sources is for identification only and does not constitute endorsement by the U.S. Department of Health and Human Services, or the U.S. Centers for Disease Control and Prevention.

Disclosure

R.H.B. is an employee of Base Pair Biotechnologies and G.W.J. is both co-founder and employee of Base Pair Biotechnologies, as such they have a financial interest in the aptamers being used commercially.

Conflict of Interest

The other authors have no conflicts of interest to declare.

1.0 Introduction

During the siege of Khirra in 600 BCE, the Athenian army used hellebore to poison the city's water source, causing the defenders to become so weak with diarrhea that the Athenians beat them quite easily (Mayor 2003). In the intervening two and a half millennia, humanity has seen no shortage of advancements in the field of chemical warfare, with several of the most widely used weapons of chemical warfare belonging to the family of organophosphorus nerve agents (OPNAs). During the cold war, sarin gas, VX, and novichok agents were produced (Vucinic et al. 2017) and stockpiled by both the United States and the USSR (Wiener and Hoffman 2004). These agents were used against Iranian and Kurdish troops during the Iran-Iraq war, and during the Persian Gulf War, OPNAs affected both combatants and civilians (Holstege et al. 1997). Even within the past two decades, OPNAs were used in several instances that resulted in thousands of civilian exposures (Kyle 1999; Rosman et al. 2014; Stone 2018). Conventional tests lack the selectivity to identify the specific OPNA used, and testing is not always readily available at the site of an exposure.

1.2 Organophosphorus Nerve Agents.

OPNAs are odorless and colorless that act by blocking the binding site of acetylcholinesterase (AChE), inhibiting the breakdown of acetylcholine (Holstege et al. 1997). The resulting buildup of acetylcholine leads to the inhibition of neural communication to muscles and glands and can lead to increased saliva and tear production, diarrhea, vomiting, muscle tremors, confusion, paralysis and even death (A. and A. 1998; Mangas et al. 2017). Long-term effects of acute organophosphorus (OP) poisoning includes low serum and erythrocyte AChE levels, neurological damage, psychiatric effects, dermatological disorders, and sleeplessness. (A. and A. 1998; Talabani et al. 2017). While the onset of symptoms is often rapid, within minutes to hours, some symptoms can take much longer to present. Diagnosis of exposure is typically based on symptoms and is often confirmed by measuring OPNA adducts to butyrylcholinesterase (BChE) in blood (Wiener and Hoffman 2004).

The effects from chronic, low level OP exposure are not usually as severe as exposure at higher levels (Ray and Richards 2001; Salvi et al. 2003), yet still include peripheral nervous system (Baker and Sedgwick 1996; Bowman et al. 1989; Dési and Nagymajtényi 1999) and respiratory damage (Hulse et al. 2014), along with depression and cognitive impairment (Phillips and Deshpande 2016). In fact, OP poisoning kills about 200,000 people annually worldwide (Gunnell et al. 2007). Since low level OP exposures do not typically evoke observable cholinergic symptoms such as lachrymation, salivation, meiosis, or muscle fasciculation, it is often difficult to access exposure based on symptoms or cholinesterase activity (Bloch-Shilderman et al. 2018). Since OPNAs are odorless and colorless (Ellison 2008), detecting occupational exposure is difficult by observational means. Further, even intermediate exposure, which results in flu-like symptoms, can represent a case where AChE inhibition never reaches a quantifiable level (Ray and Richards 2001). In short, current detection methods based either on symptoms or cholinergic activity are insufficient to confirm chronic low/mid-level exposure from OPs.

1.3 Detecting OPNA Exposure.

OPNA exposure is based on enzymatic activity testing or by detection of the OPNAs or their metabolites directly. Techniques include ELISA (Viveros et al. 2006; Walton et al. 2012), bead arrays (Du et al. 2011), engineered-nanopore technologies (Wang et al. 2009), and label-free techniques, such as surface plasmon resonance (SPR), quartz-crystal microbalance (Funari et al. 2013), wave-guided interferometry (Zourob et al. 2007), and mass spectrometry (MS) (Knaack et al. 2012). Field deployable photometric dipstick assays do exist, but these methods have limited sensitivity (10^{-7} – 10^{-5} M) (No et al. 2007), false positives, matrix-dependent sample processing (Apilux et al. 2015), or interference from sample matrices such as blood. Two commonly used OPNA exposure quantification methods include liquid chromatography coupled to tandem mass spectrometry (LC-MS/MS) and the Test-mate ChE Assay (Knaack et al. 2012; Rajapakse et al. 2011). LC-MS/MS exhibits relatively high sensitivity and specificity, yet it requires a multi-step extraction/concentration procedure (Knaack et al. 2012). LC-MS/MS methodology is not field deployable. The Test-mate ChE assay has been shown to be a promising field-kit, with a transduction method based the modified Ellman method which measures the activity of red blood cell AChE and plasma BChE (Ellman et al. 1961). This kit produces results within 4 minutes, requires ~10 μ L of blood (Rajapakse et al. 2011), yet it is based on measuring target OP proteins, AChE or BChE, not the specific OP directly. Test-mate also requires confirmatory measurement of AChE baseline activity to account for intra- and inter-person variability (Ellman et al. 1961). Recently a wearable glove biosensor has been reported, where an electrochemical sensor is printed on a disposable nitrile glove enabling “swipe sampling” of suspicious surfaces or agricultural products (Mishra et al. 2017). However, the utility of this method is difficult to assess relative to solution-phase biosensing because operation is demonstrated by coating a surface with a 200 μ M OP solution. To date, development of alternative OP detection techniques have been challenging due to sample volume requirements, poor reproducibility, specificity, or sensitivity. Furthermore, the use of surface immobilization and labeling steps make assay development and validation slow and expensive. Therefore, a free-solution assay method, represents an innovative alternative for OP detection.

1.4 The Free Solution Assay.

The OP quantification methodology reported here is a free-solution assay (FSA) (Bornhop et al. 2016) that is label-free, enzyme-free, and compatible with complex matrices. When combined with a compensated interferometer (CI) (Kammer et al. 2018), the mix-and-read measurement can be used without relative mass dependency and in native environments, allowing for therapeutic screening (Tiefenbrunn et al. 2013), improving in-vitro/in-vivo correlations for first-in-human dose estimates (Wang et al. 2017), investigating biological mechanisms of action (Luka et al. 2011), and quantifying protein biomarker targets (Olmsted et al. 2014). When combined with aptamer probes (Kammer et al. 2014), FSA(CI) enables rapid, high sensitivity (pg/mL), specific assays that enable quantification of two OPNA acids (VX and GB) in serum. The OPNAs studied here were the primary metabolites of Sarin, also known as NATO designation G-series, “B” (GB, IUPAC name (RS)-Propan-2-yl methylphosphonofluoridate), and venomous agent X (VX, IUPAC name: Ethyl({2-[bis(propan-2-yl)amino]ethyl} sulfanyl)(methyl)phosphinate).

1.4 Aptamers as probes.

Aptamers are short segments of single-strand DNA or RNA that can be quickly and inexpensively selected to bind to desired targets. They can serve as sensors (Cho et al. 2009), therapeutics (Kaur and Roy 2008), and cellular process regulators (Toulme et al. 2004), as well as drug targeting agents (Cao et al. 2009; Chu et al. 2006a; Chu et al. 2006b; Chu et al. 2006c). The diversity of applications and the varied targets to which aptamers can bind (proteins, peptides, and small molecules) stem from the ability of aptamers to form complex three-dimensional shapes including both helices and single-stranded loops. Aptamers are selected *in vitro*, are easily stored and transported, and are stable for months to years, making them potential alternatives to antibodies or enzymes. Aptamers work particularly well with FSA because the unbound aptamer undergoes a significant conformation change upon binding, resulting in a large FSA signal (Bornhop et al. 2016; Kammer et al. 2014). An added benefit is that the aptamer-target signal is produced in absence of chemical modification or labeling.

This report contains the first demonstrated use of the CI to screen probes for FSAs and high-sensitivity assays. Label-free, solution-phase operation provided rapid selection of “the best-in-class” probe for the target in the matrix of interest. Once selected, aptamer-probe binding affinity was determined to estimate performance. Best performing aptamers exhibited KD values from 16.1 ± 4.4 nM to 41.6 ± 8.3 nM, thereby allowing quantification of the target, GB acid or VX acid at the level of 31 pg/mL (224 pM) and 29 pg/mL (231 pM) respectively in 25% serum. Cross-species selectivity for either serum assay was determined rapidly, by again using a mix-and-read screen. Response from the screens reported off-target, or interfering, signals well below the limit of quantification (LOQ) of the assay for the best-in-class aptamer probe, with the off-target concentration needing to be more than a thousand times higher than the target to produce quantifiable inaccuracy at the LOQ.

2.0 Methods

2.1 Aptamer selection.

All OPNA acid aptamers were selected by Base Pair Biotechnologies, Inc. (Pearland, TX, USA). Briefly, 2-aminoethyl monophosphonate (2-AEMP, Sigma Aldrich cat. SML0706) was covalently coupled through its primary amine group to aldehyde functionalized agarose resin (ThermoFisher Aminolink™ coupling resin, cat. 20381) using the manufacturer’s recommended protocol for coupling and mild reduction using cyanoborohydride. A proprietary library of approximately 1015 unique natural DNA sequences were utilized for aptamer selection. Following three rounds of selection against the immobilized 2-AEMP, in the 4th round, we: 1) again applied the binding population of aptamers to the ligand-beads, 2) washed away weakly bound DNA species, and 3) subsequently split the pool of beads into two groups and offered one of the specific nerve agent metabolites in free solution as an elution agent and collected the resulting aptamer pool released from the beads. The eluted pools were then amplified by PCR, and the second, 5'-phosphorylated strand was digested away using lambda exonuclease. The resulting single stranded pools were then recombined for the next round of exposure to the 2-AEMP beads followed by specific elution using either VX- or GB-acid. This process of split-and- pool SELEX was repeated for 14 rounds.

All binding and wash steps were performed in 1X PBS, 1% BSA, 1 mM MgCl₂, 0.02% baker's yeast tRNA, and 0.5% Tween-20. In the 4th round and onward, decreasing concentrations of the free target molecule were offered to obtain the tightest binders. After 14 rounds, the enriched aptamer pools were labeled with unique barcodes via PCR and sequenced using an Ion Torrent PGM next-generation sequencer (Thermo Fisher). For each target, bioinformatics analysis was used to choose aptamers for synthesis and functional screening in the described assay.

2.2 Aptamer preparation.

The stock aptamers were reconstituted from the dried pellet to a concentration of 100 μ M in a modified Phosphate Buffered Saline (PBS) containing 1mM MgCl₂, 10 mM Tris HCl, and 0.1 mM EDTA with pH 7.5. All further dilutions used this PBS formulation. The stock aptamer solution was then diluted to 2 μ M (the "Working Concentration") in PBS. Once diluted to the working concentration, the aptamers were refolded by heating the solution to 90°C for 5 minutes in a water bath, then cooled to room temperature for 15 minutes. This process ensures the aptamers were in their desired conformation following lyophilizing and shipping.

2.3 OPNA acid target solution preparation.

Ethyl methylphosphonate (VX acid) with a molecular weight of 124.08 g/mol and density of 1.172 g/mL (9.4 M/L) was obtained from Synquest Laboratories (98% pure) in liquid form. A stock solution of 100 mM was prepared by diluting 10.59 μ L into 989.41 μ L of PBS. Isopropyl methylphosphonate (GB acid) with a molecular weight of 138.10 g/mol and density of 1.087 g/mL (7.87 M/L) was obtained from Sigma-Aldrich (98% pure) in liquid form. A stock solution of 100 mM GB acid was prepared by diluting 12.7 μ L in 987.3 μ L of PBS.

2.4 Aptamer Screening.

Aptamers were screened in 25% pooled human serum / 75% buffer using the FSA method to determine the signal produced by the aptamers upon binding to the target. The pooled human serum used in this work was acquired from a commercial source and did not meet the definition of human subjects as specified in 45-CFR 46.102 (f). Six aptamers were screened for GB acid and five aptamers were screened for VX acid. The screen was performed by measuring the FSA signal for a high concentration of OPNA acid (500 nM) in the absence and presence of the aptamer at a concentration of 100 nM. These solutions were prepared by first diluting the stock aptamers 1:100 in PBS to obtain a 1 μ M solution and diluting the OPNA metabolite targets 1:250,000 in PBS to obtain a 400 nM solution. The 400 nM OPNA solution was diluted in 100% pooled human serum to produce a 50% serum / 50 % PBS solution containing 200 nM of OPNA acid target. The 2 μ M aptamer solution was diluted 1:2 in PBS to obtain a 1 μ M aptamer solution. Then, 50 μ L of the 200 nM OPNA acid solution was mixed with 50 μ L of the 1 μ M aptamer solution to obtain 100 μ L of 500 nM aptamer + 100 nM OPNA acid to provide the binding sample. The reference sample was prepared by adding 50 μ L of the 1 μ M aptamer solution to 50 μ L of a 50% serum / 50% PBS solution with no OPNA acid target. Following a 30- minute equilibration at room temperature, the phase shift between binding and reference solutions for each aptamer was

measured using CI. Additionally, to correct for the potential contribution of background to the signal from the OPNA acid target in the absence of binding, the response was determined by the phase shift between 100 nM OPNA acid and a blank 25% serum / 75% PBS solution was measured and subtracted from the aptamer-binding phase shift measurements.

2.5 Affinity Characterization.

Binding affinity assays were performed in an end-point format as described previously (Kammer et al. 2014). To prepare affinity measurements in 25% serum / 75% PBS, a 7-point, 1:2 serial dilution of OPNA acid target was created in 50% serum / 50% PBS with concentrations ranging from 2000–31.25 nM (for VX 203), with a 0 nM solution prepared with just 50% serum / 50% PBS. A 400 nM aptamer solution was prepared by diluting the 2 μ M working concentration 1:5 in PBS. Then 20 μ L of each OPNA acid concentration was combined with 20 μ L of the aptamer solution to create the binding sample. 20 μ L of each OPNA acid concentration was combined with 20 μ L of blank 50% serum / 50% PBS to create the reference sample. This resulted in binding and reference samples with final OPNA acid concentrations ranging from 1000–15.6 nM and a 0 nM concentration, and an aptamer concentration of 200 nM in the binding samples only with no aptamer in the reference samples, in 25% serum. The samples were allowed to incubate at room temperature for 1 hour, then the phase shift between each concentration's reference and sample was measured. The resulting phase shift, averaged over five replicates, was plotted vs. target concentration. The 0 nM concentration sample, containing only the aptamer, compared to the reference solution (no aptamer or target) provides a measure of the background signal contribution due to the aptamer and is subtracted from all concentrations. Dissociation constants were then calculated by fitting the data to a single-site saturation isotherm using Graphpad PrismTM according to the equation:

$$y = \frac{B_{max} \cdot X}{K_D + X} \quad (1)$$

2.6 Cross Reactivity.

To assess specificity, the best performing aptamer for each target was tested for its binding to the other targets. For example, the aptamer for GB acid was tested for non-specific binding to aptamers selected for VX acid, and vice versa. This determination was performed in 25% serum using a similar procedure to the screening experiments. Here the response for the interactions was quantified for both the target and off-target OPNA acid at 0 and 1000 nM, when incubated with the respective 500 nM aptamer.

2.7 LOQ Determinations and Unknown Quantification.

Calibration curves were constructed in 25% serum / 75% PBS in a similar manner to the affinity determinations with the goal of determining the assay analytical figures of merit. A 9-point, 2:1 serial dilution was prepared in 50% serum / 50% PBS ranging from 20 nM to 0.08 nM, with two additional concentrations at 100 and 200 nM, and a zero concentration

with no OPNA acid target. The aptamer was prepared at a 1000 nM concentration in PBS. Then 20 μ L of each OPNA acid concentration was combined with 20 μ L of the aptamer solution to create the binding sample, and 20 μ L of each OPNA acid concentration was combined with 20 μ L of blank 50% serum / 50% PBS to create the reference sample. This resulted in 12 sample-reference pairs with concentrations ranging from 100 to 0 nM of the OPNA acid target, with 500 nM aptamer in the binding sample and no aptamer in the reference.

Test “unknowns” were prepared by spiking serum with a known concentration of the OPNA acid target, diluting to 50% serum in PBS, then combining equal amounts with a 1000 nM aptamer in PBS solution to serve as the binding sample and blank PBS to serve as reference. This resulted in a 25% serum solution with 500 nM aptamer in the binding sample and no aptamer in the reference. The phase shift between sample and reference was fitted to the calibration curve to recover the concentration of spiked OPNA acid target.

3.0 Results & Discussion

3.1 Aptamer Screening.

The ideal probe for a quantitative interaction assay would: 1) produce a large, reproducible signal, 2) have a high affinity to its target, and 3) exhibit little or no off-target interactions that could result in false-positive signals. One of the advantages of FSA over techniques such as ELISA is that probe-target performance can be evaluated quite rapidly using a mix-and-read screening approach. This approach is illustrated in Fig. 1, showing how a single serum sample is split into two 10 μ L aliquots, with one aliquot being combined with the probe aptamer at high concentration and the other aliquot combined with a refractive index-matched, non-binding control solution. Following a short incubation period, the FSA signal is quantified by measuring the binding sample and reference sample simultaneously in the compensated interferometer. Since FSA is matrix independent these screening determinations can be performed by simply quantifying the signal and signal/noise for a number of candidate probes in the desired milieu.

Fig. 2 illustrates the results of the FSA-CIR screening experiments for the aptamer probe candidates. Here a large concentration of the OPNA acid target (100 nM) was incubated with 500 nM of each aptamer in 25% serum (the binding sample), and 100 nM of the OPNA acid target was incubated with the 25% serum solution (the reference sample). This experiment is rapid, taking approximately 30 minutes to complete, including sample preparation, incubation and CI analysis times. This simple approach was used to identify which of the aptamer probes displayed the largest signal for each OPNA acid target. Hence, in less than an afternoon, two most attractive aptamer-probe candidates for each OPNA acid target were selected from 11 starting species. In this way, the FSA method allowed for rapid identification of the best aptamer candidates for further investigation.

As illustrated in Fig. 2A and 2B the best performing aptamers for VX acid were VX203 and VX798 (internal nomenclature), providing CI signals of 5143 ± 66 and 4113 ± 97 mrad, respectively. Screening results for the aptamers selected against GB acid are presented in Fig. 2C and 2D. Here the highest screening signal (best candidates) were the GB946 and

GB459 aptamers, with FSA-CI assay reporting signals of 1194 ± 107 mrad and 767 ± 92 mrad, respectively. Since FSA is a molecular interaction assay that measures conformation and hydration changes (solution molecular polarizability) (Bornhop et al. 2016), it has been found that noise in the measurement (background) can vary with structure and solution-phase properties, including rearrangement and self-association. Best candidates were selected for the assay by determining the S/N produced by the screening results (Fig. 2B and 2D). The S/N is an invaluable indicator of performance as illustrated by a comparison of VX798 or VX109. While both aptamers gave similar absolute CI signals (4112 vs 4436 mrad), VX798 provided nearly double the S/N (42 vs 24) over VX109, making VX798 the primary candidate probe for further analysis. The GB acid aptamer screening produced one distinct frontrunner, both in terms of CI signal and S/N, the GB946 species. Yet several other aptamers (GB048, 402 and 459) gave promising screening results. In this case, the S/N determination did not produce a clear choice for the second GB acid aptamer to advance for further testing. Because screening and S/N analysis in urine showed GB459 to be a promising candidate (data not shown) this aptamer was also advanced for further characterization

3.2 Aptamer Affinity Determinations.

To ensure the aptamer probes exhibit high affinity, a property related to selectivity, saturation isotherm binding assays were performed. These measurements also provide insight as to the potential value of the assays in the context of target quantification. The saturation isotherms for each of the two best aptamer candidates to each OPNA acid target, enabled binding affinity, KD, to the OPNA acid to be quantified. The FSA method has been used widely for KD determinations (Kussrow et al. 2012; Kussrow et al. 2009) consists of holding the aptamer concentration fixed at a value near the assumed KD, and measuring the binding signal of the OPNA acid to the aptamer as a function of concentration. As shown in Fig. 3, aptamer OPNA acid affinity measurements all yielded $R^2 > 0.9$ and affinity values with KDs all in the nanomolar range. Specifically, the VX203 aptamer yielded a KD of 35.1 ± 9.5 nM (Fig. 3A), while the alternate aptamer probe (VX798) gave a KD of 41.6 ± 8.3 nM (Fig. 3B) both determined in 25% serum. From these two candidates, VX203 was selected as the probe for quantitative assays on the merit of its larger signal and higher affinity (lower KD). Evaluation of the GB aptamer candidates yielded affinities of 37.9 ± 8.4 nM ($R^2 = 0.98$) for GB946 (Fig. 3C) and 16.1 ± 4.4 nM ($R^2 = 0.95$) for GB459 (Fig. 3D). With both candidates yielding affinities in the 10's of nanomolar, GB946 was selected as the probe aptamer due to its larger signal (4022 mrad vs 2380 mrad). Results of these binding affinity measurements indicate that two excellent candidates have been identified, upon which a high-quality serum assay for the VX and GB acids can be developed.

3.3 The Quantitative Assay.

Based on previous experience (Olmsted et al. 2014), it was hypothesized that candidate aptamer probes with affinity values in the low nanomolar range often produce assays with pM or pg/mL sensitivity with good selectivity. To confirm this hypothesis, calibration curves were constructed for the top two contenders for each target and then evaluated the assay performance with two unknowns to determine preliminary quantitative performance. Figure 4 presents the result of these calibration investigations, illustrating that the FSA-CI assays

provide excellent performance. Specifically, the LOQs, calculated as $3 \times$ standard deviation of replicate determinations/(calibration curve slope), were determined to be 231 pM (29 pg/mL) and 224 pM (31 pg/mL) for the quantification of VX acid and GB acid respectively (structures shown in Fig. 5A). Limits of detection (LODs), calculated as $3 \times$ instrument baseline standard deviation over 5-seconds/(calibration curve slope), were 23 pM (3 pg/mL) and 73 pM (10 pg/mL) for the target OPNA acids in 25% serum. The two-step, mix-and-read assay provides a dynamic range of ~ 2.5 orders of magnitude and requires just 10 μ L of serum to perform the assay with >5 replicates per concentration for the standards and unknown sample. By comparison, the most widely used techniques for high-sensitivity OPNA exposure confirmation are based on mass spectrometric detection of OPNA acids (Hamelin et al. 2014; Schulze et al. 2016), adducts to tyrosine (Crow et al. 2014), or BChE (Carter et al. 2013; Mathews et al. 2017). The protein adduct methods report a range of LODs from 18–97 pg/mL for tyrosine adducts to 350–4,000 pg/mL for BChE adducts. The LC-MS/MS LODs of OPNA acids in serum were previously reported as 400 pg/mL for GB acid and 500 pg/mL for VX acid from 50 μ L lysed blood, serum, and plasma specimens. By comparison, FSA provided an LOQ of 30 pg/mL GB acid from 10 μ L of serum, without the need for protein precipitation, digestion, or extraction steps required in LC-MS/MS methods.

Conventional LC-MS/MS quantification of OPNA acids and protein adducts remains an attractive option for confirmatory testing; however, the method described here yields a more than 130-fold improvement in sensitivity with a LOD of 2.9 pg/mL to current LC-MS/MS measurements of OPNA acids, at a fifth of the sample volume and without the need for time-consuming sample extraction steps or costly and bulky laboratory equipment.

3.4 Testing Unknowns

As part of assay development, “unknown” determinations were tested for accuracy. Two spiked unknowns were prepared for each target using spiked blank serum. This data is overlaid upon the calibration curves (open circles) in Fig. 4 and shows recovery with an average error in the determination of less than 6% (Table 1). More notably, when plotting the spiked concentration versus the determined concentration, as shown in Fig. 5B, the determined concentrations lie upon a straight line ($R^2 > 0.99$).

3.5 Cross Reactivity

Screening Finally, screening assays were performed to evaluate the specificity of the aptamer probes. In this experiment, the two top performing aptamers for each target were incubated with a high concentration of both targets (1000 nM). The results of these determinations are presented in Fig. 5C, which illustrates that for the two best aptamers, VX203 and GB946, the level of cross-reactivity is low. Specifically, VX203 and GB946 produced a signal at or below the LOQ for their respective off-targets (LOQ determined from Fig. 4). Even the 2nd best performing aptamers produced a signal near the LOQ of the respective off-target quantification assay.

For example, the LOQ for the VX assay was determined to be 231 pM, corresponding to a CI signal of 215 mrad. However, the 2nd best GB acid aptamer produced a signal of -487

mrads when incubated with the high concentration (1000 nM) of VX acid. Even if only considering the absolute magnitude of the signal, GB459 produced a signal only twice the VX acid assay LOQ despite a VX acid concentration of 4300 times higher than the LOQ. If both GB and VX acids were present in a sample at the concentration of the LOQ (231 pM), the presence of GB acid would only introduce an error of 9.5% in the quantification of VX acid. An additional metric of specificity uniquely available from the FSA method is signal directionality. In other words, when the GB acid aptamer binds VX acid, the result is a negative signal.

Likewise, the 2nd best aptamer for VX acid, VX798, produced a signal of 120 mrad when incubated with GB acid. The LOQ for the GB acid assay was determined to be 224 pM, which corresponded to a CI signal of 52 mrad. For a GB acid concentration of 4500 times the concentration of the VX acid LOQ, the VX acid aptamer only produced a signal equivalent to twice that of the GB acid LOQ. If both targets were present in equal concentration at the LOQ (224 pM), the presence of GB acid would result in a 9.9% error to the VX acid quantification.

These cross-reactivity results suggest that candidate probe aptamers would correctly report which nerve agent is present. As illustrated in Fig. 5A, VX acid and GB acid share remarkably similar chemical structures, differing by just one methyl group on the non-polar carbon chain. Given the size of the molecules and their structural similarity, the specificity of the aptamer probes (Fig. 5C) are even more noteworthy. There is a remote chance that the aptamer could interact with a different contaminant in the serum but given the magnitude of the KD values and the outcome of the cross-reactivity experiments, the likelihood of this producing a quantifiable signal that leads to a false positive is minimal.

4.0 Conclusion

FSA's mix-and-read format, combined with CI's simplicity, low cost, small size, and high level of environmental compensation paves the way for the development of a field deployable platform for quantifying exposure to chemical warfare agents. The unique transduction mechanism of FSA coupled with aptamer probes and the high sensitivity of CI, facilitated relatively simple quantitative assays for VX acid and GB acid with detection limits of 3 pg/mL of VX acid and 10 pg/mL for GB acid. The aptamer-FSA determinations are less complex than existing laboratory-based assays and 2–3 orders of magnitude below the reported detection limits mass-spectrometry based methods. FSA methodology provides freedom from aptamer probe surface immobilization or labeling, maximizing signal, while retaining binding affinity and specificity to the target. Free-solution operation also enables rapid screening of perspective probe-target pairs allowing the development of quantitative assays to be expedited.

While the need to 'index match' the sample and reference solution does provide matrix-independent operation, it does represent a potential limitation because accurate pipetting is required when preparing assay solutions. Assay speed is also somewhat limited by the need for the solutions to reach equilibrium. Yet, this is the case for any quantitative assay and there are methods to expedite the assay preparation step. Finally, the current CI is a research

(bread-board) instrument requires some fineness to align and data analysis is somewhat tedious due to the need to manually read the signal for processing.

Currently, an automated laser-capillary alignment approach and data analysis methodology (software) are under development, with the ultimate goal of making CI a user-friendly bench-top reader. Additional future work includes the expansion of the aptamer-FSA method to other OPNAs and assay validation in patient samples. The ultimate goal of these and future studies is to develop a mix-and-read assay and field-deployable reader that can be used to identify and quantify specific OPNA's at physiologically relevant levels, with high specificity, on constrained sample volumes and at reduced costs relative to existing methods.

Acknowledgements

This work was supported in part by the Centers for Disease Control and Prevention, and in part Grant No. CHE 1610964 awarded by the National Science Foundation (NSF) to DJB.

References:

- A. BM, A. BK, 1998 Review of health consequences from high-, intermediate- and low-level exposure to organophosphorus nerve agents. *Journal of Applied Toxicology* 18(6), 393–408. [PubMed: 9840747]
- Apilux A, Isarankura-Na-Ayudhya C, Tantimongcolwat T, Prachayasittikul V, 2015 Paper- based acetylcholinesterase inhibition assay combining a wet system for organophosphate and carbamate pesticides detection. *EXCLI Journal* 14, 307–319. [PubMed: 26417364]
- Baker DJ, Sedgwick EM, 1996 Single fibre electromyographic changes in man after organophosphate exposure. *Human & Experimental Toxicology* 15(5), 369–375. [PubMed: 8735458]
- Bloch-Shilderman E, Rabinovitz I, Egoz I, Yacov G, Allon N, Nili U, 2018 Determining a threshold sub-acute dose leading to minimal physiological alterations following prolonged exposure to the nerve agent VX in rats. *Archives of toxicology*. 92(2), 873,892. [PubMed: 29127449]
- Bornhop DJ, Kammer MN, Kussrow A, Flowers RA 2nd, Meiler J, 2016 Origin and prediction of free-resolution interaction studies performed label-free. *Proc Natl Acad SciUSA* 113(12), E1595–1604.nd
- Bowman PD, Schuschereba ST, Johnson TW, Woo FJ, McKinney L, Wheeler CR, Frost D, Korte DW, 1989 Myopathic changes in diaphragm of rats fed pyridostigmine bromide subchronically. *Fundamental and Applied Toxicology* 13(1), 110–117. [PubMed: 2767351]
- Cao Z, Tong R, Mishra A, Xu W, Wong GC, Cheng J, Lu Y, 2009 Reversible cell- specific drug delivery with aptamer-functionalized liposomes. *Angewandte Chemie* 48(35), 6494–6498. [PubMed: 19623590]
- Carter MD, Crow BS, Pantazides BG, Watson CM, Thomas JD, Blake TA, Johnson RC, 2013 Direct Quantitation of Methyl Phosphonate Adducts to Human Serum Butyrylcholinesterase by Immunomagnetic-UHPLC-MS/MS. *Analyticalchemistry* 85(22), 11106–11111.
- Cho EJ, Lee JW, Ellington AD, 2009 Applications of Aptamers as Sensors. *Annu Rev Anal Chem* 2, 241–264.
- Chu TC, Marks JW, Lavery LA, Faulkner S, Rosenblum MG, Ellington AD, Levy M, 2006a Aptamer : toxin conjugates that specifically target prostate tumor cells. *Cancer Res* 66(12), 5989–5992. [PubMed: 16778167]
- Chu TC, Shieh F, Lavery LA, Levy M, Richards-Kortum R, Korgel BA, Ellington AD, 2006b Labeling tumor cells with fluorescent nanocrystal-aptamer bioconjugates. *Biosens Bioelectron* 21(10), 1859–1866. [PubMed: 16495043]
- Chu TC, Twu KY, Ellington AD, Levy M, 2006c Aptamer mediated siRNA delivery. *Nucleic Acids Res* 34(10).
- Crow BS, Pantazides BG, Quinones-Gonzalez J, Garton JW, Carter MD, Perez JW, Watson CM, Tomcik DJ, Crenshaw MD, Brewer BN, Riches JR, Stubbs SJ, Read RW, Evans RA, Thomas JD,

- Blake TA, Johnson RC, 2014 Simultaneous Measurement of Tabun, Sarin, Soman, Cyclosarin, VR, VX, and VM Adducts to Tyrosine in Blood Products by Isotope Dilution UHPLC-MS/MS. *Analytical chemistry* 86(20), 10397–10405. [PubMed: 25286390]
- Dési I, Nagymajtényi L, 1999 Electrophysiological biomarkers of an organophosphorous pesticide, dichlorvos. *Toxicology Letters* 107(1), 55–64. [PubMed: 10414781]
- Du D, Wang J, Wang L, Lu D, Smith JN, Timchalk C, Lin Y, 2011 Magnetic Electrochemical Sensing Platform for Biomonitoring of Exposure to Organophosphorus Pesticides and Nerve Agents Based on Simultaneous Measurement of Total Enzyme Amount and Enzyme Activity. *Analytical chemistry* 83(10), 3770–3777. [PubMed: 21462919]
- Ellison DH, 2008 Handbook of chemical and biological warfare agents, 2nd ed. CRC Press, Boca Raton.nd
- Ellman GL, Courtney KD, Andres V, Featherstone RM, 1961 A new and rapid colorimetric determination of acetylcholinesterase activity. *Biochemical Pharmacology* 7(2), 88–95. [PubMed: 13726518]
- Funari R, Della Ventura B, Schiavo L, Esposito R, Altucci C, Velotta R, 2013 Detection of Parathion Pesticide by Quartz Crystal Microbalance Functionalized with UV-Activated Antibodies. *Analytical chemistry* 85(13), 6392–6397. [PubMed: 23721081]
- Gunnell D, Eddleston M, Phillips MR, Konradsen F, 2007 The global distribution of fatal pesticide self-poisoning: Systematic review. *BMC Public Health* 7(1), 357. [PubMed: 18154668]
- Hamelin EI, Schulze ND, Shaner RL, Coleman RM, Lawrence RJ, Crow BS, Jakubowski EM, Johnson RC, 2014 Quantitation of five organophosphorus nerve agent metabolites in serum using hydrophilic interaction liquid chromatography and tandem mass spectrometry. *Analytical and bioanalytical chemistry* 406(21), 5195–5202. [PubMed: 24633507]
- Holstege CP, Kirk M, Sidell FR, 1997 CHEMICAL WARFARE: Nerve Agent Poisoning. *Critical Care Clinics* 13(4), 923–942. [PubMed: 9330846]
- Hulse EJ, Davies JOJ, Simpson AJ, Sciuto AM, Eddleston M, 2014 Respiratory Complications of Organophosphorus Nerve Agent and Insecticide Poisoning. Implications for Respiratory and Critical Care. *American Journal of Respiratory and Critical Care Medicine* 190(12), 1342–1354. [PubMed: 25419614]
- Kammer MN, Kussrow AK, Olmsted IR, Bornhop DJ, 2018 A Highly Compensated Interferometer for Biochemical Analysis. *ACS sensors*.
- Kammer MN, Olmsted IR, Kussrow AK, Morris MJ, Jackson GW, Bornhop DJ, 2014 Characterizing aptamer small molecule interactions with backscattering interferometry. *The Analyst* 139(22), 5879–5884. [PubMed: 25229067]
- Kaur G, Roy I, 2008 Therapeutic applications of aptamers. *Expert Opin Inv Drug* 17(1), 43–60.
- Knaack JS, Zhou Y, Abney CW, Jacob JT, Prezioso SM, Hardy K, Lemire SW, Thomas J, Johnson RC, 2012 A High-Throughput Diagnostic Method for Measuring Human Exposure to Organophosphorus Nerve Agents. *Analytical chemistry* 84(21), 9470–9477. [PubMed: 23083472]
- Kussrow A, Enders CS, Bornhop DJ, 2012 Interferometric Methods for Label-Free Molecular Interaction Studies. *Analytical chemistry* 84(2), 779–792. [PubMed: 22060037]
- Kussrow A, Kaltgrad E, Wolfenden ML, Cloninger MJ, Finn MG, Bornhop DJ, 2009 Measurement of monovalent and polyvalent carbohydrate-lectin binding by back-scattering interferometry. *Analytical chemistry* 81(12), 4889–4897. [PubMed: 19462965]
- Kyle BO, 1999 Aum Shinrikyo: Once and Future Threat? *Emerging Infectious Disease journal* 5(4), 413.
- Luka Z, Moss F, Loukachevitch LV, Bornhop DJ, Wagner C, 2011 Histone Demethylase LSD1 Is a Folate-Binding Protein. *Biochemistry-U S* 50(21), 4750–4756.
- Mangas I, Estevez J, Vilanova E, França TCC, 2017 New insights on molecular interactions of organophosphorus pesticides with esterases. *Toxicology* 376, 30–43. [PubMed: 27311923]
- Mathews TP, Carter MD, Johnson D, Isenberg SL, Graham LA, Thomas JD, Johnson RC, 2017 High-Confidence Qualitative Identification of Organophosphorus Nerve Agent Adducts to Human Butyrylcholinesterase. *Analytical chemistry* 89(3), 1955–1964. [PubMed: 28208252]
- Mayor A, 2003 Greek fire, poison arrows, and scorpion bombs : biological and chemical warfare in the ancient world, 1st ed. Overlook Duckworth, Woodstock.

- Mishra RK, Hubble LJ, Martin A, Kumar R, Barfidokht A, Kim JY, Musameh MM, Kyratzis IL, Wang J, 2017 Wearable Flexible and Stretchable Glove Biosensor for On- Site Detection of Organophosphorus Chemical Threats. *ACS sensors* 2(4), 553–561. [PubMed: 28723187]
- No H-Y, Kim YA, Lee YT, Lee H-S, 2007 Cholinesterase-based dipstick assay for the detection of organophosphate and carbamate pesticides. *Anal Chim Acta* 594(1), 37–43. [PubMed: 17560383]
- Olmsted IR, Hassanein M, Kussrow A, Hoeksema M, Li M, Massion PP, Bornhop DJ, 2014 Toward Rapid, High Sensitivity, Volume-Constrained Biomarker Quantification and Validation using Backscattering Interferometry. *Analytical chemistry* in press.
- Phillips KF, Deshpande LS, 2016 Repeated low-dose organophosphate DFP exposure leads to the development of depression and cognitive impairment in a rat model of Gulf War Illness. *NeuroToxicology* 52, 127–133. [PubMed: 26619911]
- Rajapakse BN, Thiermann H, Eyer P, Worek F, Bowe SJ, Dawson AH, Buckley NA, 2011 Evaluation of the Test-mate ChE (Cholinesterase) Field Kit in Acute Organophosphorus Poisoning. *Annals of Emergency Medicine* 58(6), 559–564.e556. [PubMed: 22098995]
- Ray DE, Richards PG, 2001 The potential for toxic effects of chronic, low-dose exposure to organophosphates. *Toxicology Letters* 120(1), 343–351. [PubMed: 11323193]
- Rosman Y, Eisenkraft A, Milk N, et al., 2014 Lessons learned from the syrian sarin attack: Evaluation of a clinical syndrome through social media. *Annals of Internal Medicine* 160(9), 644–648. [PubMed: 24798526]
- Salvi RM, Lara DR, Ghisolfi ES, Portela LV, Dias RD, Souza DO, 2003 Neuropsychiatric Evaluation in Subjects Chronically Exposed to Organophosphate Pesticides. *Toxicological Sciences* 72(2), 267–271. [PubMed: 12660361]
- Schulze ND, Hamelin EI, Winkeljohn WR, Shaner RL, Basden BJ, deCastro BR, Pantazides BG, Thomas JD, Johnson RC, 2016 Evaluation of Multiple Blood Matrices for Assessment of Human Exposure to Nerve Agents. *J Anal Toxicol* 40(3), 229–235. [PubMed: 26861671]
- Stone R, 2018 U.K. attack puts nerve agent in the spotlight. *Science* 359(6382), 1314–1315. [PubMed: 29567684]
- Talabani JM, Ali AI, Kadir AM, Rashid R, Samin F, Greenwood D, Hay AWM, 2017 Long-term health effects of chemical warfare agents on children following a single heavy exposure. *Human & Experimental Toxicology* 37(8), 836–847. [PubMed: 29069930]
- Tiefenbrunn T, Forli S, Baksh MM, Chang MW, Happer M, Lin YC, Perryman AL, Rhee JK, Torbett BE, Olson AJ, Elder JH, Finn MG, Stout CD, 2013 Small Molecule Regulation of Protein Conformation by Binding in the Flap of HIV Protease. *ACS chemical biology* 8(6), 1223–1231. [PubMed: 23540839]
- Toulme JJ, Di Primo C, Boucard D, 2004 Regulating eukaryotic gene expression with aptamers. *Febs Lett* 567(1), 55–62. [PubMed: 15165893]
- Viveros L, Paliwal S, McCrae D, Wild J, Simonian A, 2006 A fluorescence-based biosensor for the detection of organophosphate pesticides and chemical warfare agents. *Sensors and Actuators B: Chemical* 115(1), 150–157.
- Vucinic S, Antonijevic B, Tsatsakis AM, Vassilopoulou L, Docea AO, Nosyrev AE, Izotov BN, Thiermann H, Drakoulis N, Brkic D, 2017 Environmental exposure to organophosphorus nerve agents. *Environmental Toxicology and Pharmacology* 56, 163–171. [PubMed: 28942081]
- Walton I, Davis M, Munro L, Catalano VJ, Cragg PJ, Huggins MT, Wallace KJ, 2012 A Fluorescent Dipyrinone Oxime for the Detection of Pesticides and Other Organophosphates. *Organic Letters* 14(11), 2686–2689. [PubMed: 22594956]
- Wang D, Zhao Q, Zoysa R.S.S.d., Guan X, 2009 Detection of nerve agent hydrolytes in an engineered nanopore. *Sensors and Actuators B: Chemical* 139(2), 440–446.
- Wang MM, Kussrow AK, Ocana MF, Chabot JR, Lepsy CS, Bornhop DJ, O'Hara DM, 2017 Physiologically relevant binding affinity quantification of monoclonal antibody PF-00547659 to mucosal addressin cell adhesion molecule for in vitro in vivo correlation. *British Journal of Pharmacology* 174(1), 70–81. [PubMed: 27760281]
- Wiener SW, Hoffman RS, 2004 Nerve Agents: A Comprehensive Review. *Journal of Intensive Care Medicine* 19(1), 22–37. [PubMed: 15035752]

Zourob M, Simonian A, Wild J, Mohr S, Fan X, Abdulhalim I, Goddard NJ, 2007 Optical leaky waveguide biosensors for the detection of organophosphorus pesticides. *The Analyst* 132(2), 114–120. [PubMed: 17260070]

Author Manuscript

Author Manuscript

Author Manuscript

Author Manuscript

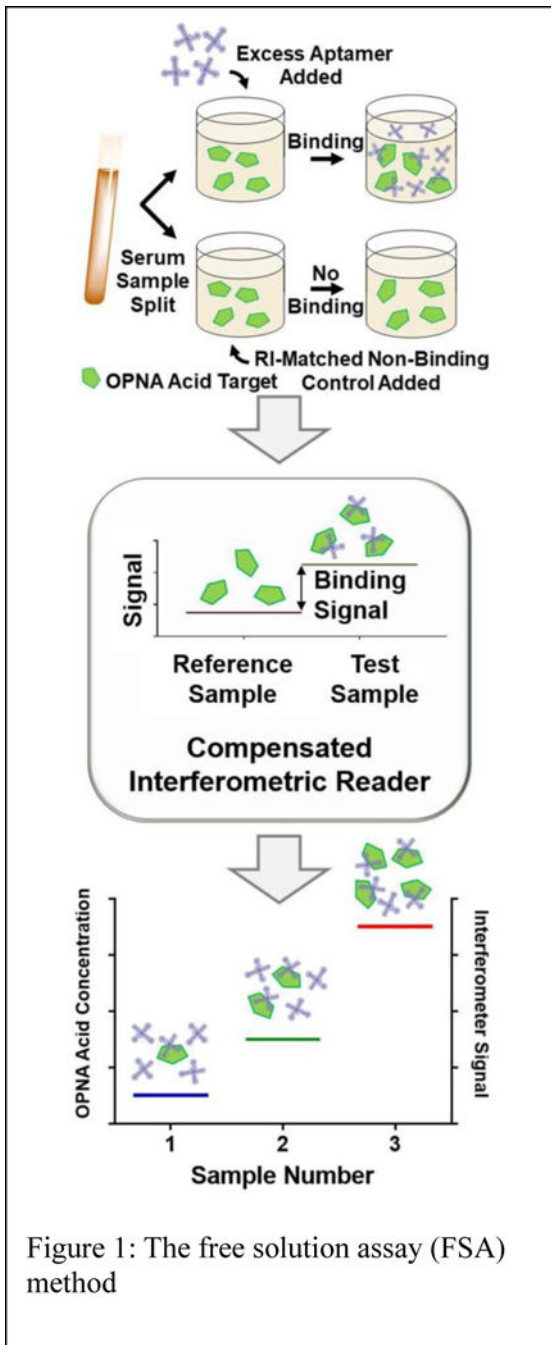


Figure 1: The free solution assay (FSA) method

Figure 1:
The free solution assay (FSA) method

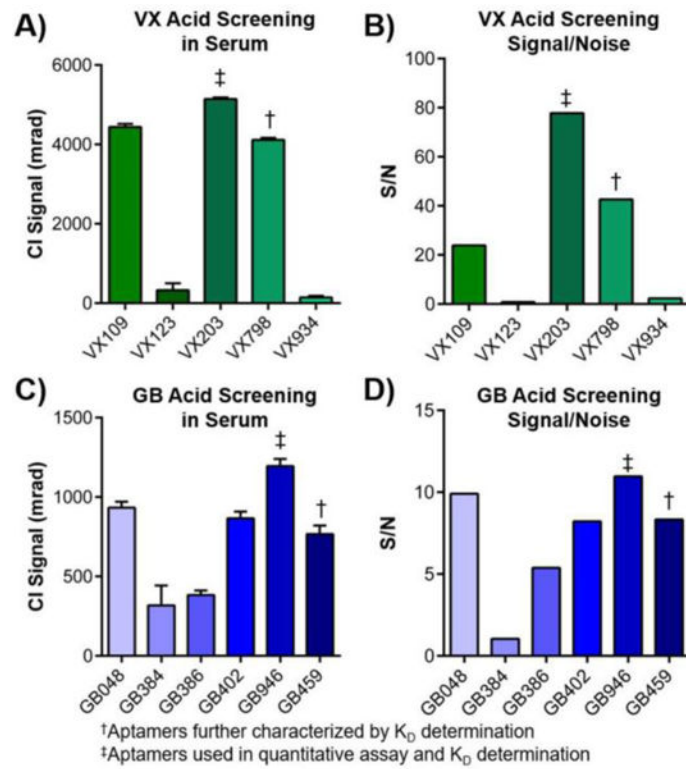


Figure 2: Screening results in serum for 11 aptamers. A) CI signal and B) signal-to-noise for VX acid binding to five aptamers. C) CI signal and D) signal-to-noise for GB acid binding to six aptamers.

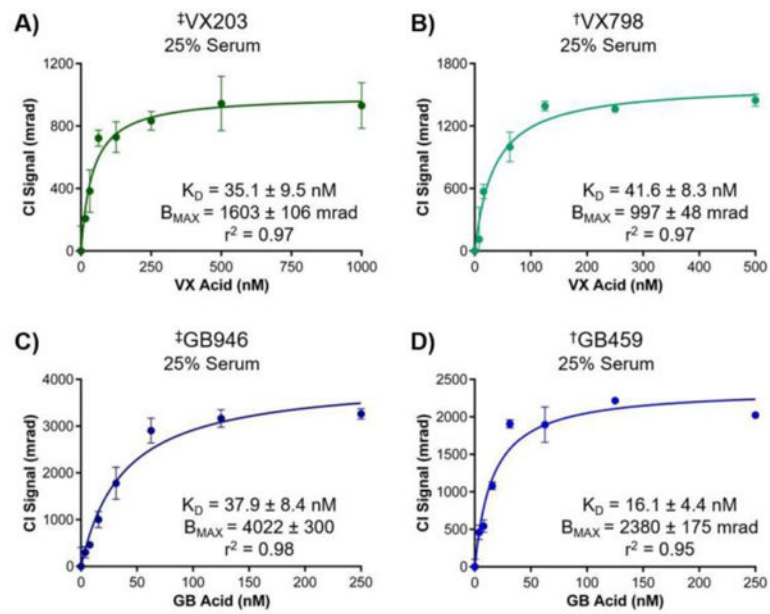


Figure 3: Binding affinities in serum. Saturation isotherm for VX Acid binding the aptamer VX203 (A) and the aptamer VX798 (B) in serum. Binding affinity saturation isotherm for GB Acid binding the aptamer GB946 (C) and the aptamer GB459 (D) in serum.

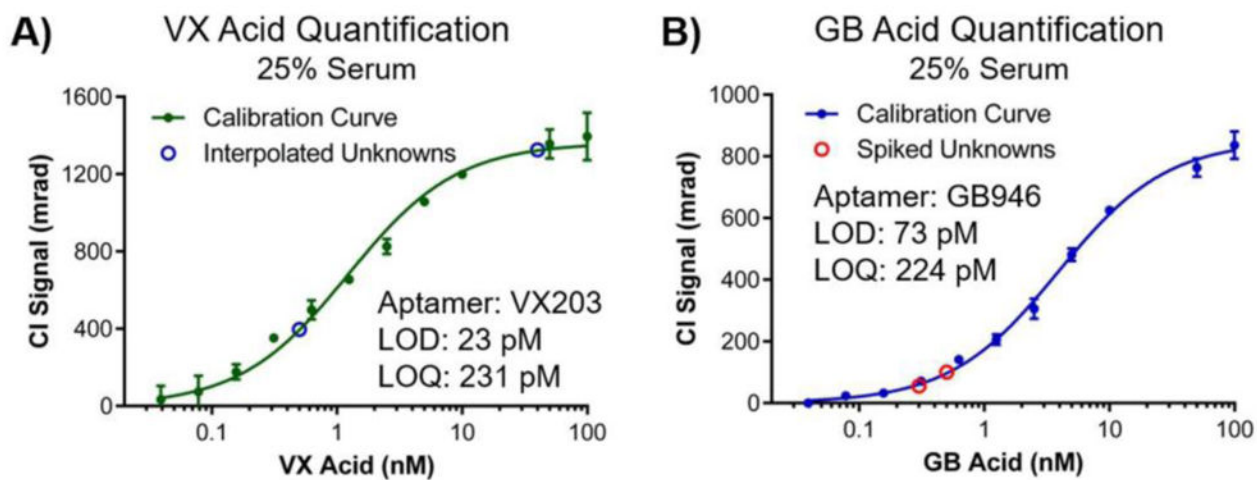


Figure 4:
Calibration curves for VX (A) and GB (B) acid quantification.

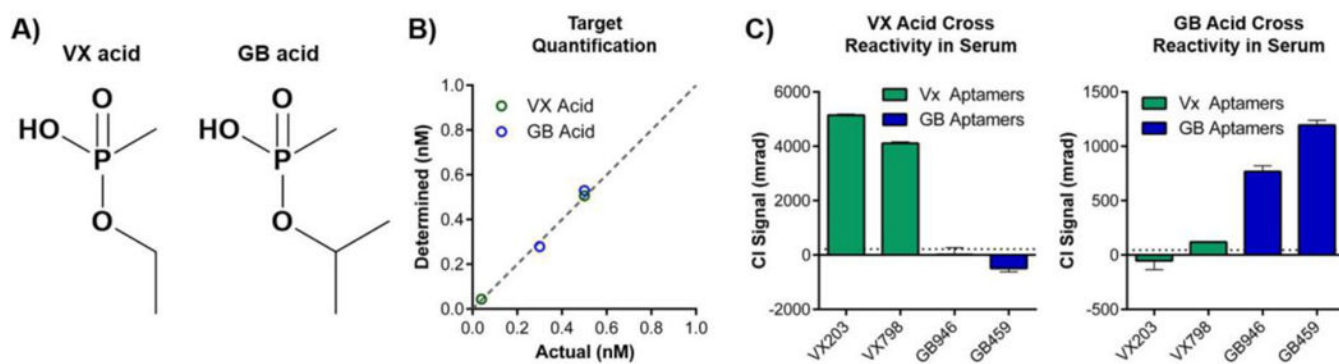


Figure 5:

A) Chemical structures of VX acid and GB acid. B) “Unknown” quantification using the best-in-class aptamer provides high accuracy determinations. C) Cross reactivity measurements tested the signal resulting from the best performing aptamers selected for both species incubated with VX acid and GB acid.

Table1

Comparison of LODs and LOQs, and FSA quantification of unknowns (values in pM)

Target	FSA	LC-MS/MS ¹	FSA Unknown Determination		
	LOD/LOQ	LOD/LOQ	Spiked Concentration	Determined Concentration ²	Error
VX Acid	23/231 pM	4000/ ³ pM	500	506 ± 29	1%
			40	43.6 ± 19	9%
GB Acid	73/224 pM	3000/ ³ pM	300	279 ± 39	7%
			500	530 ± 16	6%

¹(Schulze et al. 2016)²Average ± standard deviation of 6 replicates³No LOQ for direct OPNA measurement reported